Contents lists available at SciOpen

Food Science and Human Wellness

journal homepage: https://www.sciopen.com/journal/2097-0765

China Food Publishing Co.

The impact of Cistanche on the therapeutic potential of acne after fermentation with *Beauveria bassiana*

Xingjiang Zhang[a], Pan Wang[a], Yunwei Hu[a], Hui Ke[a], Rui Wang[a], Xiaoya Zhang[a], Huiyun Wu[a], Baiyi Chi[a], Yuyo Go[b], Xi Hui Felicia Chan[c], Qing Huang[a,*], Jianxin Wu[a,*]

[a] *Skin Health and Cosmetic Development & Evaluation Laboratory, China Pharmaceutical University, Nanjing 211198, China*
[b] *Royal Victoria Hospital, Belfast BT12 6BA, United Kingdom*
[c] *Acute Mental Health Inpatient Centre, Belfast BT9 7YG, United Kingdom*

ARTICLE INFO

Article history:
Received 8 April 2024
Received in revised form 21 April 2024
Accepted 23 September 2024

Keywords
Cistanche
Fermentation
Beauveria bassiana
Acne
Decaffeoylacteoside

ABSTRACT

Phenylethanol glycosides (PhGs) constitute crucial bioactive compounds in Cistanche Herba. However, their bioavailability is notably low. Research indicates that intestinal flora can metabolize PhGs into small polyphenols, enhancing bioavailability and pharmacological activities. In this paper, for the first time, a single strain, *Beauveria bassiana*, was found to be effective in converting PhGs from the crude extract of *Cistanche tubulosa* into small molecule polyphenols like hydroxytyrosol (HT), decaffeoylacteoside (HT-glu-rha), and caffeic acid through fermentation. We assessed the impact of pre- and post-fermentation on *Propionibacterium acnes*-induced acne related to a Western diet through *in vitro* cellular experiments. Both pre- and post-fermentation exhibited efficacy in inhibiting inflammation, oxidative stress, and mitochondrial membrane damage in *P. acnes*-induced HaCaT. Moreover, post-fermentation, unlike pre-fermentation, displayed stronger and a dose-dependent reduction in insulin-stimulated lipid synthesis in sebaceous gland cells. To further understand the increased efficacy of fermentation in inhibiting lipid synthesis, we investigated HT-glu-rha, the predominant small molecules produced during fermentation. It was shown that the compound inhibited lipid synthesis by decreasing gene expression of sterol regulatory element binding transcription factor 1 (SREBP-1) and peroxisome proliferator activated receptor gamma (PPARγ) in sebaceous gland cells.

1. Introduction

Cistanche Herba is a parasitic plant thriving in arid regions across Asia and Africa. With a long history in traditional Chinese medicine, it has served as a tonic and aphrodisiac for centuries. This herb is widely embraced as a health food supplement in Japan, China, and several Southeast Asian nations[1].

Cistanche Herba and its phenylethanol glycosides (PhGs) have been reported to exhibit various pharmacological effects, such as neuroprotection[2], immune regulation[3], antiaging[4], anti-osteoporosis[5], liver protection[6], etc. Among the PhGs, echinacoside are the most abundant and studied compounds in *Cistanche tubulosa*[7]. However, one of the major challenges of using echinacoside as oral drugs is their low bioavailability. A previous pharmacokinetic study showed that the absolute bioavailability (*F*, %) of echinacoside was only 0.83%[8]. This means that only a small fraction of the ingested echinacoside can reach the systemic circulation and exert their pharmacological effects. It is well known that prior to being absorbed into blood, many oral drugs are transformed by intestinal bacteria in gastrointestinal tract[9]. These gut flora play a key role in the digestive process, and some of them have the ability to metabolize PhGs into smaller compounds that are more easily absorbed[10]. For instance, echinacoside, when metabolized by intestinal bacteria, breaks down into smaller compounds such as hydroxytyrosol (HT), caffeic acid, verbascoside, and decaffeoylacteoside (HT-glu-rha)[11]. These metabolites exhibit

* Corresponding authors at: Skin Health and Cosmetic Development & Evaluation Laboratory, China Pharmaceutical University, Nanjing 211198, China
E-mail address: wujianxin@cpu.edu.cn (J.X. Wu); huangqing@cpu.edu.cn (Q. Huang)
Peer review under responsibility of Beijing Academy of Food Sciences.

SciOpen Publishing services by Tsinghua University Press

http://doi.org/10.26599/FSHW.2024.9250393

enhanced biological activity compared and bioavailability to their parent compounds[12]. This could elucidate why echinacoside presents low *F* but demonstrates notable biological activity. Therefore, *in vitro* microbial transformation of PhGs to improve their bioavailability and pharmacological activity deserves further study.

Fermented foods or medicinal materials have higher efficacy and utilization than unfermented ones. Fermentation can deglycosylate some glycosidic compounds, making them into smaller, more absorbable, and more permeable non-glycosidic compounds[13]. For instance, lactic acid bacteria (*Lactiplantibacillus plantarum*) has the capacity to transform relatively less biologically active flavonoid glycosides such as hesperidin and naringin into more active aglycones, namely hesperetin and naringenin. Both *in vitro* and *in vivo* studies have demonstrated the enhanced cellular transport and increased bioactivity of the fermented citrus extract[14].

Beauveria bassiana is a medicinal fungus that grows on silkworm carcasses. For centuries, infected silkworms have been utilized in Asian medicine as a tonic and immunomodulator, and was described in "Sheng Nong's herbal classic"[15]. *B. bassiana* is generally considered safe for humans, animals, and other non-target organisms[16] and performs efficient biotransformation of natural compounds and xenobiotics[17]. Recent human exposure risk assessments of some of its metabolites have further confirmed its safety for human use[18]. A blend of plant extracts underwent fermentation by *B. bassiana* and was evaluated for its impact on chicken embryo blood vessels. The fermentation process transformed glucogallin into gallic acid within the mixture, resulting in reduced toxicity and enhanced antiangiogenic properties[19].

In this study, we found for the first time that a single strain of *B. bassiana* can biotransform PhGs into small molecule polyphenols, whereas most of the previous studies have focused on the transformation of PhGs in intestinal flora. Moreover, the transformation of *B. bassiana* is similar to the metabolites produced by PhGs in human metabolism and intestinal flora, and has the potential for large-scale fermentation production. We used the fermentation product in the treatment of acne and showed good therapeutic potential *in vitro*. It provides a theoretical basis for the use of Cistanche herbs in beauty and skin care.

2. Materials and methods

2.1 Materials and chemicals

The crude extract from *C. tubulosa* was provided by Prof. Pengfei Tu of Peking University (Beijing, China). The extraction and purification process are broadly as follows: 50 g of the sample was weighed and reflux extracted twice, each for 1 h, with 600 mL of 70% ethanol. Dynamic adsorption was performed using HPD-100 resin, and the sample was eluted with a 50% ethanol solution. After recovering the ethanol under reduced pressure, the dried powder was obtained by freeze-drying using a freeze-dryer. HT, caffeic acid, verbascoside, isoacteoside and HT-glu-rha, all with the purity of over 98% were purchased from Chengdu Push Bio-technology Co., Ltd. (Sichuan, China). *B. bassiana* were obtained from China Center of Industrial Culture Collection CICC (Beijing, China). Insulin was procured from Solarbio Life Sciences (Beijing, China), and Cell Counting Kit-8 (CCK-8) was obtained from Vazyme (Nanjing, China).

2.2 Fermentation and sample collection

Inoculate the *B. bassiana* into Shah's glucose liquid medium under aseptic condition, and cultivate it under 28 ℃ condition with 200 r/min shaking bed for 2 days to make the first-grade seeds, and the $OD_{600\ nm}$ value of the optical density of *B. bassiana* suspension at the end of the cultivation reaches about 0.8; Secondary seed culture: according to the volume ratio of Shah's glucose liquid medium for 10% of the inoculum, the first level of seed inoculation into the 200 mL conical flask at 28 ℃, stirring speed of 200 r/min, culture for 2 days, to produce the second level of seed. Put 0.3 g crude extract from *C. tubulosa* into 200 mL secondary seed liquid, and incubate at 28 ℃ with stirring speed of 200 r/min. Among these, BJJ (*B. bassiana* alone for 12 days in medium without crude extract), BJJF (*B. bassiana* in medium containing crude extract for 12 days), and PHG (crude extract dissolved in medium without *B. bassiana*).

2.3 Qualitative liquid chromatography-mass spectrometry (LC-MS/MS) analysis

The compounds in the crude extracts before and after fermentation were characterized using a Waters ACQUITY UPLC I-CLASS Plus/Xeve G2-XS Q TOF instrument. This instrument incorporated a Waters ACQUITY UPLC BEH-C_{18} column (2.1 mm × 100 mm, 1.8 μm) and a mobile phase consisting of 2 constituents: 0.1% formic acid (FA) in water (A) and 0.1% FA in acetonitrile (ACN) (B). Operating at a flow rate of 0.3 mL/min, the column was maintained at a temperature of 40 °C, while the sample chamber temperature was regulated at 4 °C. Samples were detected by absorption with a wavelength range of 190−400 nm, with an inject volume of 5 μL.

The mobile phase was programmed as follows: an isocratic elution of 2%−4% B for the first 5 min, followed by a linear gradient elution of 4%−13% B from 5 to 8.5 min, 13%−18% B from 8.5 to 10 min, 18% B from 10 to 12 min, 18%−40% B from 12 to 15 min, 40%−100% B from 15 to 15.5 min. After holding the solvent composition of 100% B for the next 2 min, the gradient was returned to its starting conditions.

Mass spectrometry analysis was performed using two ionization modes: electron source ionization (ESI^+) and electron capture source ionization (ESI^-). A source voltage of 3.0 kV and a source temperature of 450 °C were applied to generate ions in both modes. An acquisition mass range of 50−1 200 Da was utilized. A cone voltage of 50 L/h and an acquisition time of around one second per spectrum were employed during the analysis. After the data acquisition using Q-TOF, the raw data were imported and processed (peak alignment, detection and identification) using the MSDIAL software system. The software determined the retention time and *m/z* data for each peak.

2.4 Quantitative LC-ultraviolet detection (UV) analysis

LC experiments were conducted using a Shimadzu (Kyoto, Japan) HPLC system consisting of an LC-20ADXR binary pump, an SIL-20ACXR autosampler, a CTO-10AS VP column oven and an SPD-20A. Chromatographic separation of analytes was achieved using a DIKMA Diamonsil C_{18} (4.6 mm × 250 mm, 5 μm) analytical column (DIKMA, Beijing, China). The column and autosampler tray temperatures were set at 30 and 4 ℃, respectively.

A mobile phase composed of eluent A (0.1% FA in water, *V/V*) and B (ACN) with a gradient elution was employed for the separation. The mobile phase was programmed as follows: an isocratic elution of 2%−4% B for the first 15 min, followed by a linear gradient elution of 4%−13% B from 15 to 25 min, 13%−18% B from 25 to 30 min, 18% B from 30 to 44 min, 18%−40% B from 44 to 53 min, 40%−100% B from 53 to 53.01 min. After holding the solvent composition of 100% B for the next 3 min, the gradient was returned to its starting conditions. The flow rate was 1.0 mL/min, and samples were detected by absorption at 280 and 330 nm, with an inject volume of 20 μL.

2.5 Cell culture

The immortalized human sebaceous (Yansheng Industrial Co., Ltd., Shanghai, China) gland cell line (Sebocytes) was used. Human keratinocytes (HaCaT) were obtained from Meisen Cell Technology Co., Ltd. Sebocytes and HaCaT cells were incubated in complete Dulbecco's modified Eagle's medium (DMEM; Meisen Cell Technology Co., Hangzhou, China) containing 100 U/mL penicillin, streptomycin (100 μg/mL), and 10% fetal bovine serum (FBS, TransGen Biotech, Beijing, China).

2.6 Cell viability assay

Cell viability was assessed through a standard CCK-8 assay (Vazyme). Sebocytes and HaCaT cells were subjected to drug treatment post-adherence to the dish bottom. Following a 24-h incubation, 10% CCK-8 reagent was introduced into each well. After 2 h of incubation at 37 °C, the optical density was gauged at a wavelength of 450 nm using a SpectraMax 190 plate reader (Molecular Devices Corporation, CA, USA). The outcomes were expressed as relative to the control.

2.7 Nile red staining

Sebocytes were treated with Nile red to visualize intracellular lipid deposition. Post Nile red staining for 10 min, along with DAPI staining for cell nuclei, the stained cells were examined using a fluorescence microscope (MShot, Wuhan, China). Additionally, Sebocytes were suspended in 500 μL Dulbecco's phosphate-buffered saline (DPBS, Sigma-Aldrich, Shanghai, PR China), and their fluorescence intensity was measured using a flow cytometer (FACScalibur, Becton Dickinson, San Josè, CA, USA).

2.8 Microbial cultivation

Propionibacterium acnes (ATCC 6919) was procured from the China Industrial Culture Preservation Centre (Beijing, China). *P. acnes* was cultured anaerobically in solid and liquid fortified *Clostridium difficile* medium (Hopebiol, Shandong, China) at 37 °C for 72 h. This suspension was heat-treated at 80 °C, and the resulting heat-killed bacteria were employed in a previously documented stimulation experiment[20]. The collected bacterial pellet was eventually suspended in serum-free medium, achieving a bacterial concentration of 1.2×10^9 CFU/mL.

2.9 Intracellular reactive oxygen species (ROS) detection assay intracellular

ROS levels were assessed using 2′,7′-dichlorodihydrofluorescein diacetate (DCFH-DA) (Beyotime, Shanghai, China). DCFH-DA at 5 μmol/L was added to each well and incubated at 37 °C for 0.5 h. The cells were then washed with DPBS (Sigma-Aldrich), suspended, and analyzed using a CytoFLEX Flow cytometer.

2.10 Mitochondrial membrane potential assay

The mitochondrial membrane potential was assessed with the fluorescent probe JC-1 (Beyotime). JC-1 generates red fluorescence in mitochondria with normal membrane potentials by forming aggregates. Conversely, in damaged or depolarized mitochondria, JC-1 forms monomers that emit green fluorescence. Cells were exposed to DMEM containing 5 μmol/L JC-1 for 15 min at 37 °C, and subsequent imaging was conducted using a fluorescence microscope (MShot).

2.11 Real-time reverse transcriptase-polymerase chain reaction

Total ribonucleic acid (RNA) was extracted from cells employing RNA-easy Isolation Reagent (Vazyme). Subsequently, RNA was reverse transcribed to complementary DNA (cDNA) using the HiScript III 1st Strand cDNA Synthesis Kit (+gDNA wiper) (Vazyme). For quantitative polymerase chain reaction (qPCR), ChamQ Universal SYBR qPCR Master Mix (Vazyme) containing a fluorescent dye was utilized. The RT-qPCR analysis was conducted on a real-time PCR Detection system (Bioer, Hangzhou, China). All primer sequences were sourced from GenScript (Nanjing, China).

3. Result

3.1 Characterization of the chemical compounds in PHG and the metabolites in BJJF

The UPLC-Q-TOF-MS system was utilized to identify the chemical constituents in both PHG and BJJF (Figs. 1A-B). Referring to a previous study[21], we identified a total of 38 compounds, with 30 of them being PhGs (Table 1). Specifically, we noted 6 compounds in BJJF (dehydrogenated decaffeoylacteoside, HT, HT-glu-rha,

Table 1
Sequences of primers.

Genes	Forward primer (5′–3′)	Reveres primer (5′–3′)
β-Actin	TGGCACCCAGCACAATGAA	CTAAGTCATAGTCCGCCTAGAAGCA
PPARγ	GCCAAGCTGCTCCAGAAAAT	TGATCACCTGCAGTAGCTGCA
SREBP-1	GGAGCCATGGATTGCACTTT	TCAAATAGGCCAGGGAAGTCA
IL-6	GCAGAAAACAACCTGAACCTT	ACCTCAAACTCCAAAAGACCA
IL-1α	CAATTGTATGGACTGCCCAAG	ATAGTTCTTAGTGCCGTGAGTT

caffeic acid sulfate conjugation, caffeic acid, and hydroxylated verbascoside) frequently documented in research on PhGs metabolism *in vivo*. These compounds originate from the parent compound through processes such as hydroxylation, sulfonation, or ester bond breaking. Additionally, we observed a parent ion at *m/z* 655.187 3 and secondary ion fragments at *m/z* 461.166 6 and 179.035 0. These ions are probably to represent a double-hydroxylated compound of verbascoside (*m/z* 623.201 8), which has not been previously found in literature or CAS SciFinder, potentially indicating a new class of compounds. The introduction of additional hydroxyl groups is a common strategy employed by nature to enhance the stability, solubility, and biological activities of these aromatic compounds[22]. For instance, oxidized resveratrol demonstrates enhanced pharmacological activities compared to resveratrol in areas such as tyrosinase inhibition[23], anti-glycosylation[24], and anti-tumor effects[25]. Furthermore, we observed increased peak areas of small molecule PhGs like cistanoside G, cistanoside I, cistanoside F, and cistanoside H following fermentation. In positive ionization mode, we identified 2 specific metabolites of *B. bassiana*—oosporein and beauvericin, which exhibits antioxidant[26] and antibacterial properties[27].

3.2 Analysis of metabolic pathways and the contents of compounds in the BJJF

The results from our sampling at different time points to analyze substance content in the samples are presented in Table 2. In the initial fermentation stage, spanning from 0 to 6 days, we observed the conversion of echinacoside into verbascoside, indicating the presence of robust glucosidase in the culture broth. Simultaneously, a fraction of verbascoside and isoacteoside transformed into HT-glu-rha and caffeic acid. In the later stage, from 6 to 12 days, verbascoside underwent partial hydroxylation and partial transformation into HT-glu-rha and caffeic acid (Fig. 1C). The unequal presence of HT-glu-rha and caffeic acid is due to the sulfation of caffeic acid in one portion, possibly accompanied by partial oxidation during fermentation. The fermentation progression is illustrated in Fig. 2.

3.3 Effects of PHG and BJJF on P. acnes-stimulated HaCaT cells

HaCaT cell viability was assessed using CCK8 after 24 h of incubation with either PHG or BJJF. The increased dosage of PHG/BJJF (0.5%−2%, *V/V*) didn't result in significant changes (Fig. 3A).

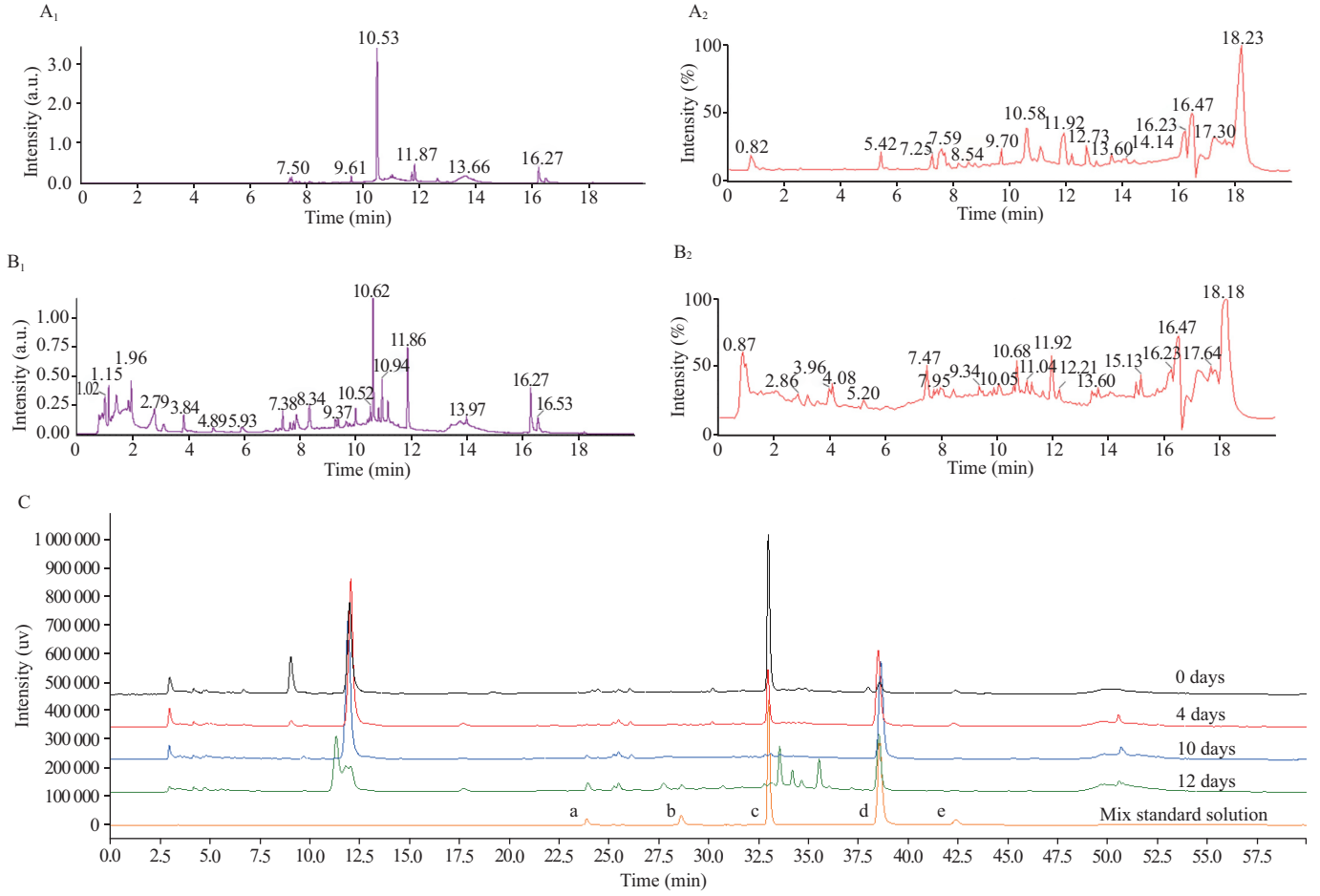

Fig. 1 Total ion chromatograms and UPLC chromatogram at UV 280 nm of PHG (A) and BJJF (B). (C) HPLC chromatograms of *B. bassiana* fermentation crude extract at different time points. In the mixed standard solution, the components are labeled as follows: a, HT-glu-rha; b, caffeic acid; c, echinacoside; d, verbascoside; e, isoacteoside.

Table 2
Compounds detected in PHG and BJJF by UPLC-Q-TOF-MS.

No.	Compounds	Retention time (min)	Ion mode	*m/z*	Molecular formula	Error ($\times 10^{-6}$)	MS/MS fragments (*m/z*)	Peak area	
								PHG	BJJF
1	Kankansose	1.23	$[M-H]^-$	649.193 0	$C_{27}H_{38}O_{18}$	−8.47	305.083 4, 135.046 0	8.2×10^3	5.0×10^5
2	Dehydrogenated decaffeoylacteoside	3.45	$[M-H]^-$	459.149 9	$C_{20}H_{28}O_{12}$	−1.96	151.040 6	1.0×10^6	6.0×10^6
3	HT	4.67	$[M-H]^-$	153.055 5	$C_8H_{10}O_3$	−1.31	123.044 9	0.0	3.8×10^6
4	6-Deoxycatalpol	7.47	$[M-H]^-$	345.118 9	$C_{15}H_{22}O_9$	−0.58	345.118 3, 299.113 3	8.2×10^7	1.8×10^5
5	HT-glu-rha	7.47	$[M-H]^-$	461.169 6	$C_{20}H_{30}O_{12}$	8.02	315.108 9, 153.060 4	8.5×10^6	3.1×10^8
6	Cistantubulose A1	7.54	$[M-H]^-$	649.198 3	$C_{27}H_{38}O_{18}$	−0.31	649.198 5, 623.220 2, 537.181 2, 335.089 6, 179.036 0	2.2×10^8	1.8×10^6
7	Adoxosidic acid	7.71	$[M-H]^-$	375.129 8	$C_{16}H_{24}O_{10}$	0.27	213.076 8	8.5×10^7	1.1×10^6
8	Caffeic acid sulfate conjugation	8.00	$[M-H]^-$	258.992 6	$C_9H_8O_7S$	3.09	167.035 1, 135.045 1	2.6×10^5	3.6×10^8
9	Androsin	8.34	$[M-H]^-$	327.107 8	$C_{15}H_{20}O_8$	−2.14	251.055 4, 179.034 9, 131.070 9	1.3×10^6	9.3×10^4
10	Caffeic acid	8.41	$[M-H]^-$	179.036 1	$C_9H_8O_4$	6.14	134.037 2	1.1×10^7	2.2×10^8
11	Cistanoside G	8.46	$[M-H]^-$	445.171 3	$C_{20}H_{30}O_{11}$	−0.45	375.130 7, 195.068 5	1.2×10^7	1.9×10^7
12	Cistanoside I	8.93	$[M-H]^-$	471.150 7	$C_{21}H_{28}O_{12}$	−0.21	369.110 4, 163.038 8	1.3×10^6	7.8×10^6
13	Cistantubuloside C1	9.70	$[M-H]^-$	801.245 1	$C_{35}H_{46}O_{21}$	−1.00	251.055 7, 195.065 6	1.8×10^8	1.8×10^6
14	Hydroxylated verbascoside	10.46	$[M-H]^-$	639.193 1	$C_{29}H_{36}O_{16}$	0.00	495.150 4, 179.035 0	1.0×10^8	8.6×10^7
15	Campneoside II	10.51	$[M-H]^-$	639.192 9	$C_{29}H_{36}O_{16}$	−0.31	621.182 7, 461.165 9, 161.025 0	1.0×10^8	9.2×10^7
16	Echinacoside	10.58	$[M-H]^-$	785.250 7	$C_{35}H_{46}O_{20}$	−0.38	785.250 7, 623.215 8, 153.091 7	1.4×10^8	8.4×10^5
17	Cistanoside F	10.68	$[M-H]^-$	487.145 8	$C_{21}H_{28}O_{13}$	0.21	179.036 8, 135.045 2	1.0×10^5	3.2×10^7
18	Dihydroxylated verbascoside	10.75	$[M-H]^-$	655.187 3	$C_{29}H_{36}O_{17}$	−1.07	487.145 9, 461.166 6, 179.035 0	6.9×10^5	6.7×10^8
19	Kankanosides K1/K2	11.09	$[M-H]^-$	815.261 0	$C_{36}H_{48}O_{21}$	−0.61	499.181 5, 197.795 3	2.0×10^7	2.1×10^6
20	Dihydroxylated verbascoside	11.22	$[M-H]^-$	655.187 4	$C_{29}H_{36}O_{17}$	−0.92	487.145 5, 323.077 4, 179.035 0	2.1×10^5	5.1×10^8
21	Kankanoside N	11.56	$[M-H]^-$	345.155 1	$C_{16}H_{26}O_8$	−1.16	113.023 4	4.9×10^6	7.6×10^4
22	Crenatoside	11.97	$[M-H]^-$	621.182 4	$C_{29}H_{34}O_{15}$	−0.16	461.166 7, 179.034 9	1.5×10^7	1.7×10^7
23	erbascoside	11.97	$[M-H]^-$	623.201 8	$C_{29}H_{36}O_{15}$	5.94	469.136 6, 461.166 7, 315.1079, 161.024 5	2.8×10^7	3.8×10^8
24	Kankanoside A	11.97	$[M-H]^-$	345.155 4	$C_{16}H_{26}O_8$	−0.29	179.034 9	1.9×10^7	9.1×10^4
25	Isoacteoside	12.73	$[M-H]^-$	623.200 8	$C_{29}H_{36}O_{15}$	4.33	461.166 2, 161.024 3	2.6×10^7	1.7×10^6
26	Cistanoside H	12.80	$[M-H]^-$	503.177 8	$C_{22}H_{32}O_{13}$	1.59	461.164 8, 375.136 1, 315.081 8	9.2×10^3	5.7×10^6
27	Tubuloside A	12.85	$[M-H]^-$	827.259 6	$C_{37}H_{48}O_{21}$	−2.30	623.197 8, 621.182 1, 469.133 2, 161.024 3	8.3×10^6	4.2×10^4
28	Campneoside	13.43	$[M-H]^-$	653.209 2	$C_{30}H_{38}O_{16}$	0.77	461.167 3, 443.155 6, 145.029 6	4.4×10^5	1.3×10^7
29	Isocistanoside C	13.79	$[M-H]^-$	637.213 7	$C_{30}H_{38}O_{15}$	−0.16	179.034 7, 161.024 2	3.7×10^7	7.8×10^6
30	Isosyringalide 3′-*α*-*L*-rhamnopyranoside	13.90	$[M-H]^-$	607.202 9	$C_{29}H_{36}O_{14}$	−0.49	461.164 5, 315.091 1, 145.031 4	1.1×10^7	3.8×10^6
31	Tubuloside B	14.02	$[M-H]^-$	665.210 0	$C_{31}H_{38}O_{16}$	1.95	503.176 5, 305.067 0, 161.024 2	8.1×10^7	1.4×10^8
32	Plantainoside C	14.26	$[M-H]^-$	637.212 0	$C_{30}H_{38}O_{15}$	−2.82	445.151 6, 145.029 1	2.5×10^6	1.1×10^6
33	2′-Acetylacteosid	14.43	$[M-H]^-$	665.208 4	$C_{31}H_{38}O_{16}$	−0.45	503.176 3, 161.024 2	7.2×10^7	4.3×10^6
34	SalsasideF	14.55	$[M-H]^-$	649.213 1	$C_{31}H_{38}O_{15}$	−1.08	503.175 4, 347.167 0, 161.024 3	3.4×10^6	2.2×10^7
35	Osmanthuside B6	15.13	$[M-H]^-$	591.208 0	$C_{29}H_{36}O_{13}$	−0.51	161.023 7	3.9×10^6	1.9×10^7
36	Eutigoside A	16.13	$[M-H]^-$	445.153 4	$C_{23}H_{26}O_9$	6.74	145.030 5, 163.041 6	3.3×10^6	7.9×10^5
37	Oosporein	1.52	$[M+Na]^+$	329.029 6	$C_{14}H_{10}O_8$	8.51	254.024 9	0.0	2.0×10^4
38	Beauvericin	10.63	$[M+K]^+$	822.372 3	$C_{45}H_{57}N_3O_9$	−0.36	663.306 0, 262.149 9, 245.137 0, 244.130 6, 134.096 5	0.0	1.4×10^4

Table 3
Contents (μg/mL) of compounds and metabolites in BJJF with *B. bassiana* at different time points ($n = 5$).

Conmpound	Time (day)						
	0	2	4	6	10	11	12
HT-glu-rha	< Limit of detection (LOD)	< LOD	11.313 ± 0.748	15.239 ± 0.896	27.524 ± 2.371	53.150 ± 3.278	75.030 ± 2.393
Caffeic acid	< LOD	< LOD	< LOD	< LOD	< LOD	5.395 ± 0.609	8.104 ± 0.176
Echinacoside	346.389 ± 12.915	251.963 ± 11.096	97.738 ± 10.954	< LOD	< LOD	< LOD	< LOD
Verbascoside	32.559 ± 1.186	120.310 ± 8.067	246.452 ± 17.087	316.568 ± 15.073	307.057 ± 9.294	228.559 ± 3.194	158.846 ± 3.545
Isoacteoside	14.256 ± 0.614	15.797 ± 0.580	13.985 ± 0.446	10.585 ± 0.896	< LOD	< LOD	< LOD

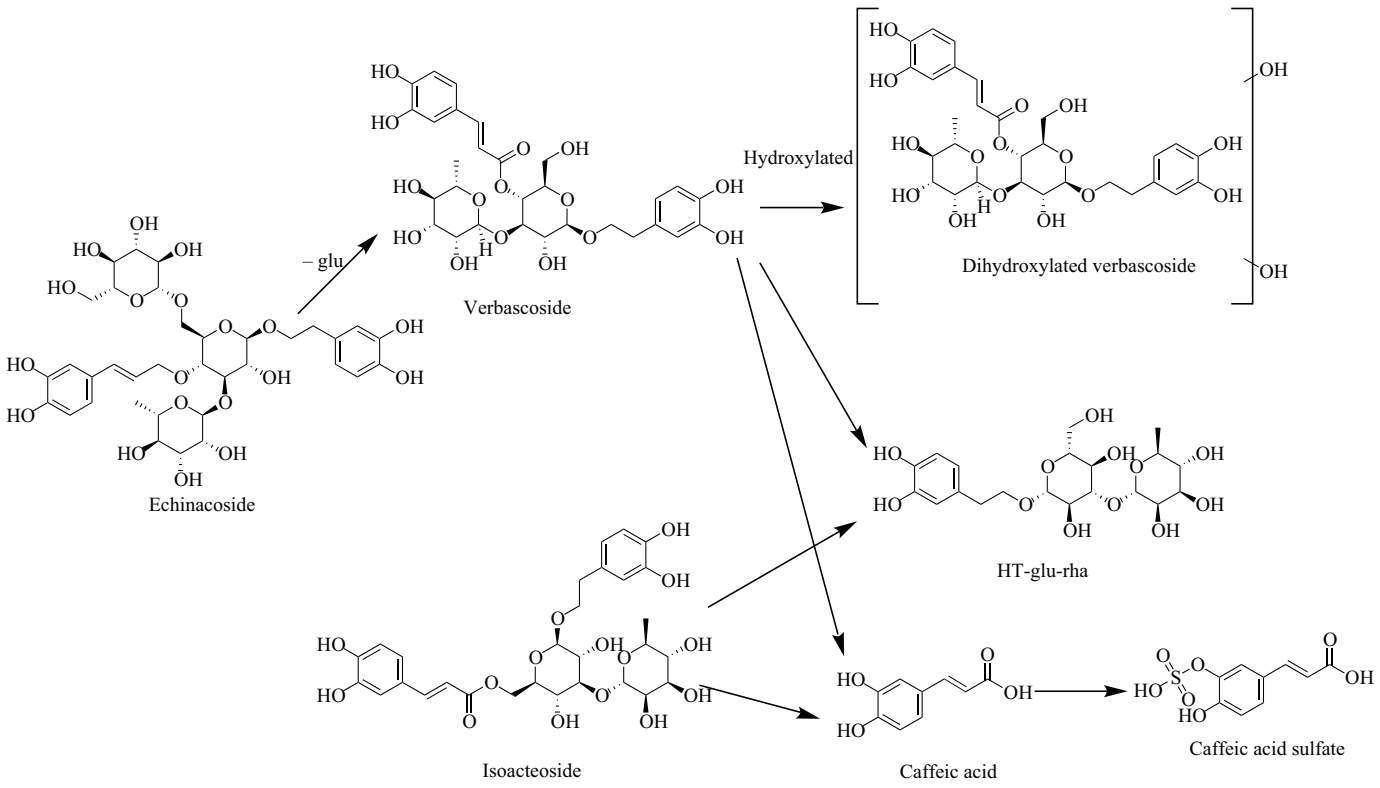

Fig. 2 Clarifications on the metabolic pathways of echinacoside, verbascoside, and isoacteoside.

P. acnes plays a key role in acne's development, initiating inflammation by triggering ROS production and releasing inflammatory cytokines[28]. HaCaT cells were cultured in 6-well plates and treated with PHG or BJJF, with or without *P. acnes*, for 24 h. Figs. 3B-C illustrate that both PHG and BJJF at dosages of 0.5%−1% (*V/V*) reduced the gene expression of *P. acnes*-induced inflammatory factors interleukin-1α (*IL-1α*) and interleukin-6 (*IL-6*) in a dose-dependent manner. Notably, the 0.25%−0.5% dose of BJJF was more effective than the 0.25%−0.5% dose of PHG in inhibiting *IL-1α* gene expression. Analyses of green fluorescence intensity *via* flow cytometry showed that both PHG and BJJF reduced ROS production in *P. acnes*-stimulated HaCaT cells. BJJF exhibited superior performance in reducing ROS at all doses, notably at 1% (Fig. 3D). Moreover, JC-1 staining indicated that both PHG and BJJF prevented the decline in mitochondrial membrane potential induced by *P. acnes* (Fig. 3E).

3.4 Effects of BJJ and HT-glu-rha on P. acnes-stimulated HaCaT cells

The increased dosage of BJJ (0.25%−1%, *V/V*) did not result in significant changes in cell viability, as measured by CCK8, after 24 h of incubation with HaCaT cells (Fig. 4A). In HaCaT cells stimulated by *P. acnes*, there was a tendency for ROS production and the expression of *IL-1α* and *IL-6* genes to decrease with increasing BJJ concentration, although this decrease was not statistically significant (Figs. 4B-D). The cell viability of HaCaT was unaffected by 0.75−12 μg/mL of HT-glu-rha (Fig. 4E). HT-glu-rha dose-dependently reduced ROS production, as well as *IL-1α* and *IL-6* gene expression in HaCaT cells stimulated by *P. acnes* (Figs. 4F-H).

3.5 Effects of PHG and BJJF on insulin-stimulated sebocytes

Sebocytes' survival was evaluated using the CCK8 assay after 24 h of incubation with either PHG or BJJF. Different concentrations of PHG/BJJF (ranging from 0.5% to 2%, *V/V*) did not exhibit significant changes (Fig. 5A). While examining cytofluorescence using Nile red dye, a significant increase in the count of intracellular lipid droplets was noted after 24 h of insulin treatment. BJJF (concentrations ranging from 0.5% to 1% (*V/V*)) displayed a concentration-dependent inhibition of insulin-induced lipogenesis. However, PHG did not exhibit an inhibition of insulin-induced lipogenesis (Fig. 5B). The fluorescence microscopy, which involved co-staining with Nile red and DAPI, produced consistent results as observed in flow cytometry (Fig. 5C).

3.6 Impact of HT-glu-rha on insulin-stimulated sebocytes and an exploration of the underlying mechanism

The cell viability of sebocytes was unaffected by 0.75−12 μg/mL of HT-glu-rha and 0.25%−1% of BJJ (Figs. 6A and C). HT-glu-rha, a compound largely generated by the fermentation. From the structure point of view, HT-glu-rha incorporates a rhamnose and a glucose into the HT core, enhancing HT's stability to a certain extent. Our research indicates that HT-glu-rha, within the range of 0.75−12 μg/mL, can dose-dependently reduce sebocyte lipid synthesis, unlike BJJ (Figs. 6B and D). Through qPCR, we observed that HT-glu-rha treatment led to a dose-dependent decrease in the gene expression of sterol regulatory element binding transcription factor 1 (*SREBP-1*) and peroxisome proliferator activated receptor gamma (*PPARγ*) in

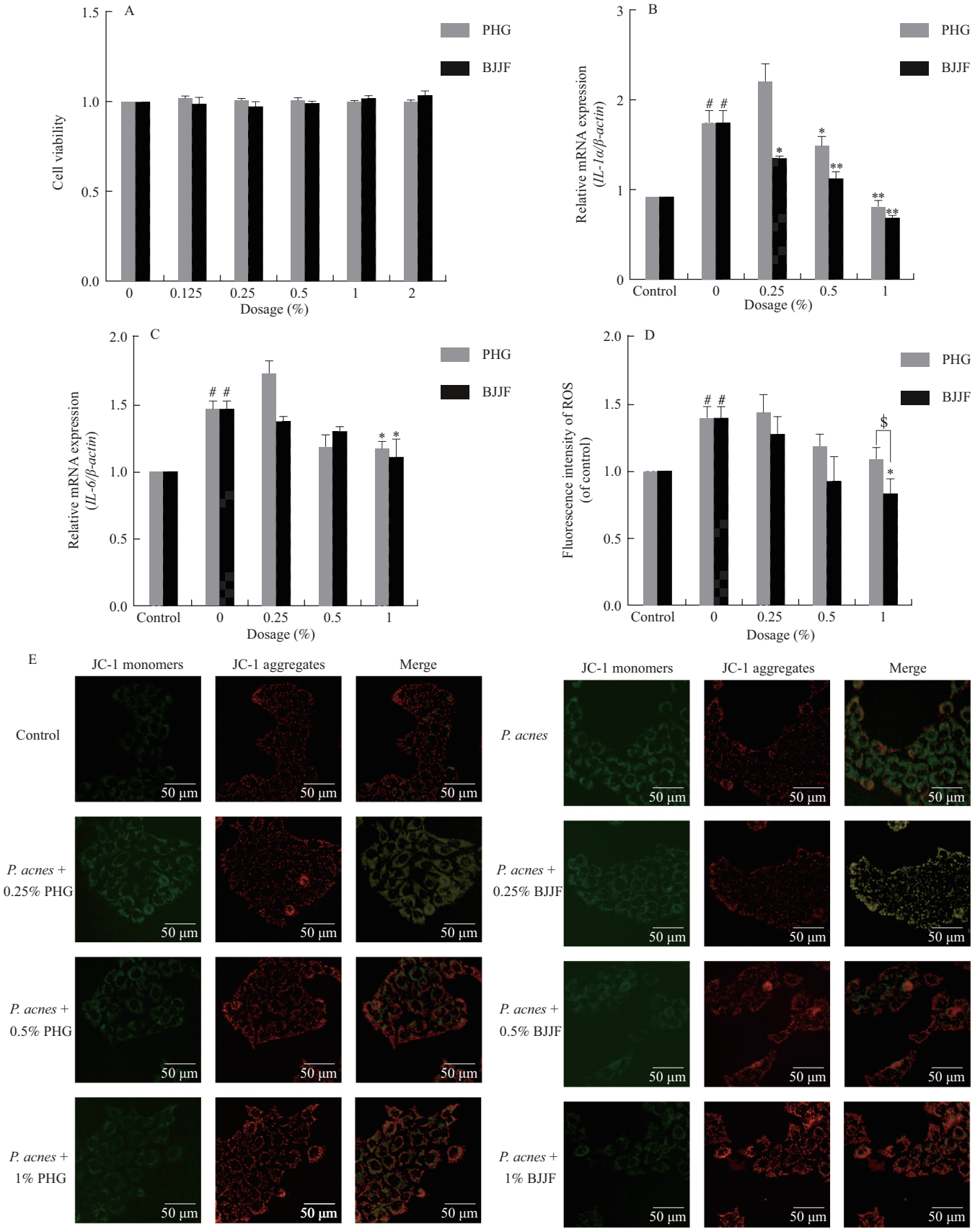

Fig. 3 PHG and BJJF reduce the damage caused by *P. acnes* to HaCaT cells. (A) Cell viability was determined by CCK8 assay. (B-C) The mRNA expression of *IL-1α* and *IL-6* was detected using RT-qPCR. (D) ROS levels were quantified as mean fluorescence intensity relative to that in the control group. (E) JC-1 staining was used for assessing mitochondrial membrane potential. Scale bar = 50 μm. All data were expressed as means ± SEM ($n = 3$). $^{\#}P < 0.05$ *vs*. control group, $^{*}P < 0.05$ and $^{**}P < 0.01$ *vs*. *P. acnes*-induced group, $^{\$}P < 0.05$ *vs*. 1% PHG group.

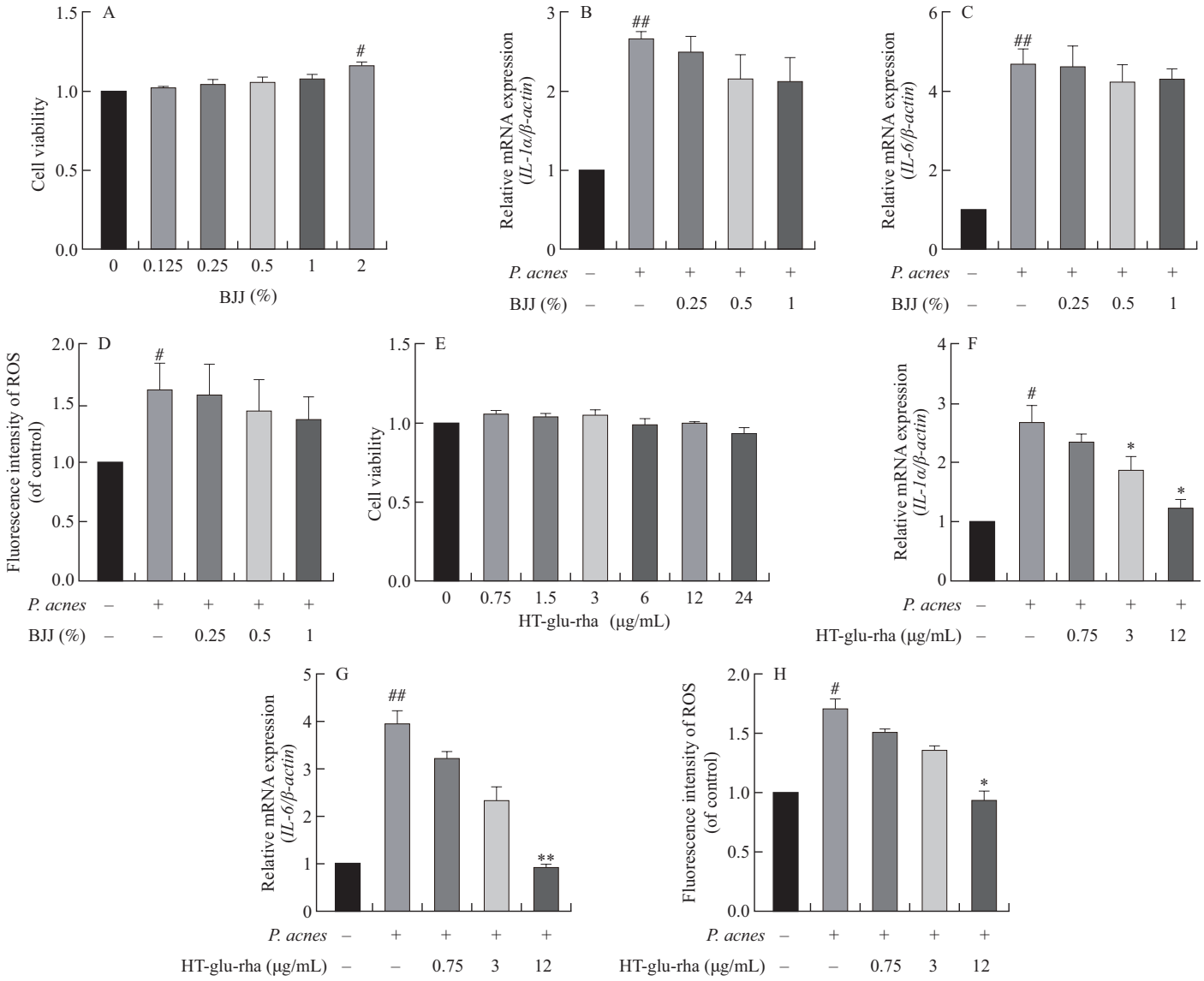

Fig. 4 BJJ and HT-glu-rha exert effects on *P. acnes*-stimulated HaCaT cells. Cell viability after BJJ (A) and HT-glu-rha (E) treatment was determined by the CCK8 assay. The mRNA expression of *IL-1α* and *IL-6* was detected using RT-qPCR after BJJ (B-C) and HT-glu-rha (F-G) treatments. ROS levels were quantified as mean fluorescence intensity relative to that in the control group using flow cytometry after treatments with BJJ (D) and HT-glu-rha (H). All data were expressed as means ± SEM ($n = 3$). $^{\#}P < 0.05$ and $^{\#\#}P < 0.01$ *vs.* control group, $^{*}P < 0.05$ and $^{**}P < 0.01$ *vs. P. acnes*-induced group.

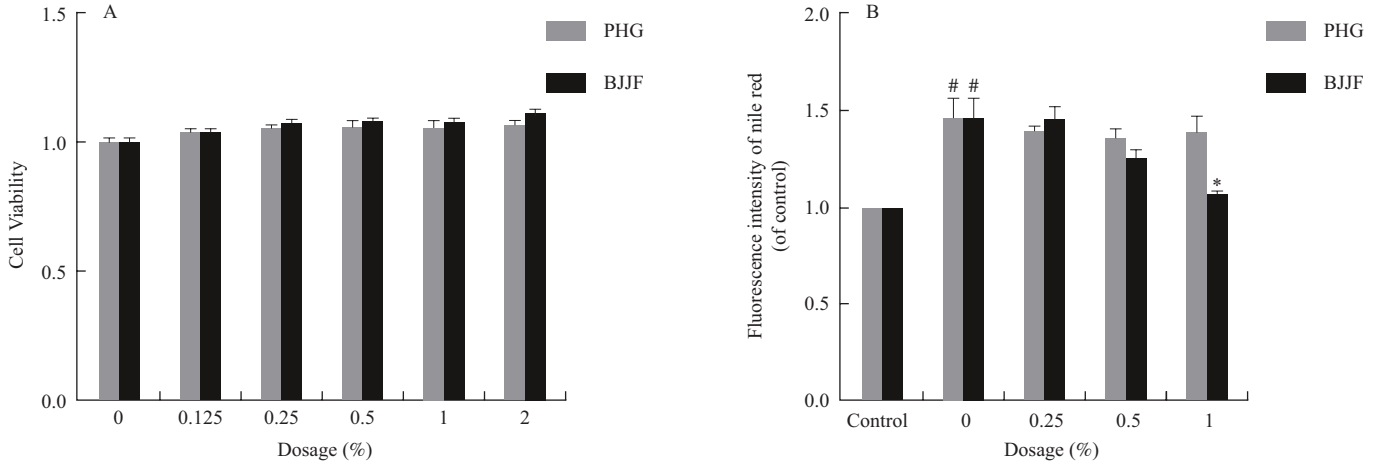

Fig. 5 PHG and BJJF's impact on insulin-induced lipid synthesis in sebaceous gland cells. (A) Cell viability was determined by CCK8 assay. (B) Using a flow cytometer, the neutral lipid contents were determined after being stained with Nile red. (C) Red fluorescence indicates neutral lipids stained with Nile red, and blue fluorescence indicates the position of cell nuclei stained with DAPI. All data were expressed as means ± SEM ($n = 3$). $^{\#}P < 0.05$ *vs.* control group, $^{*}P < 0.05$ *vs.* insulin-stimulated group.

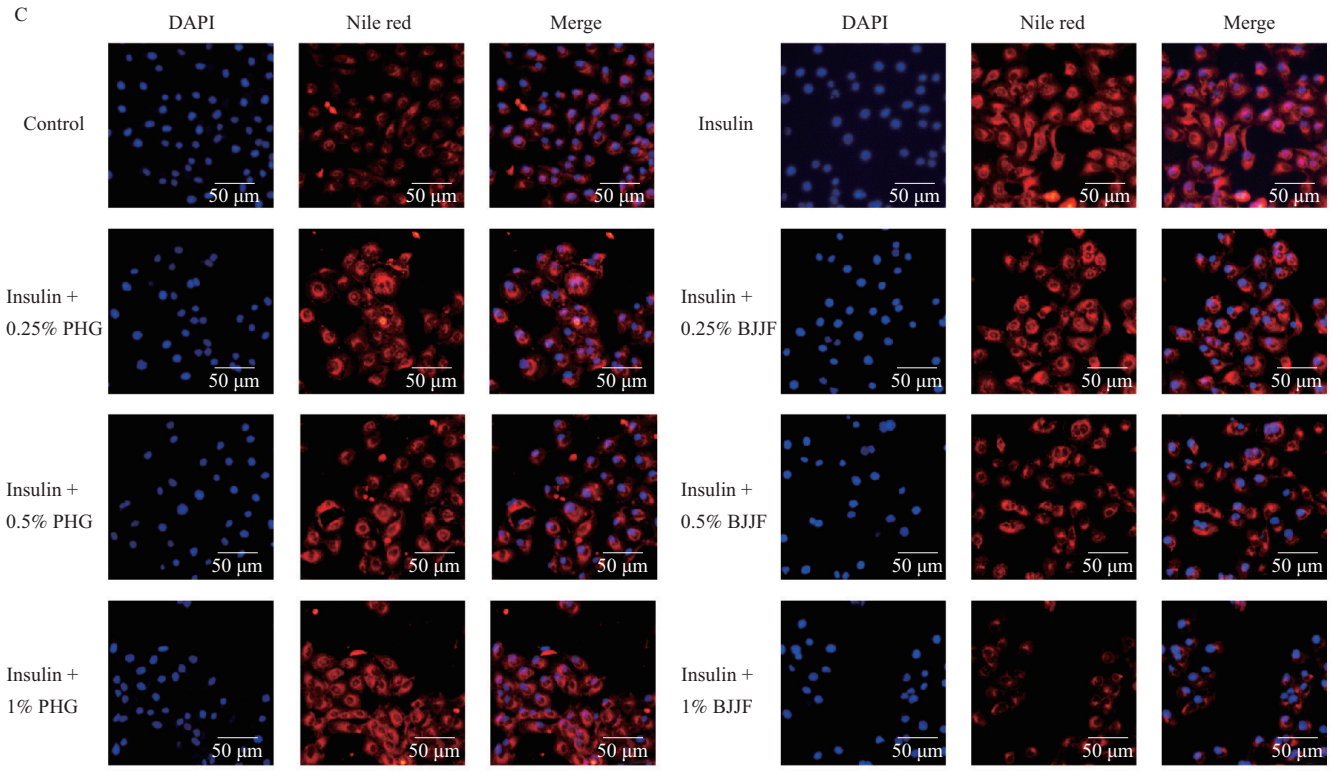

Fig. 5 (*Continued*)

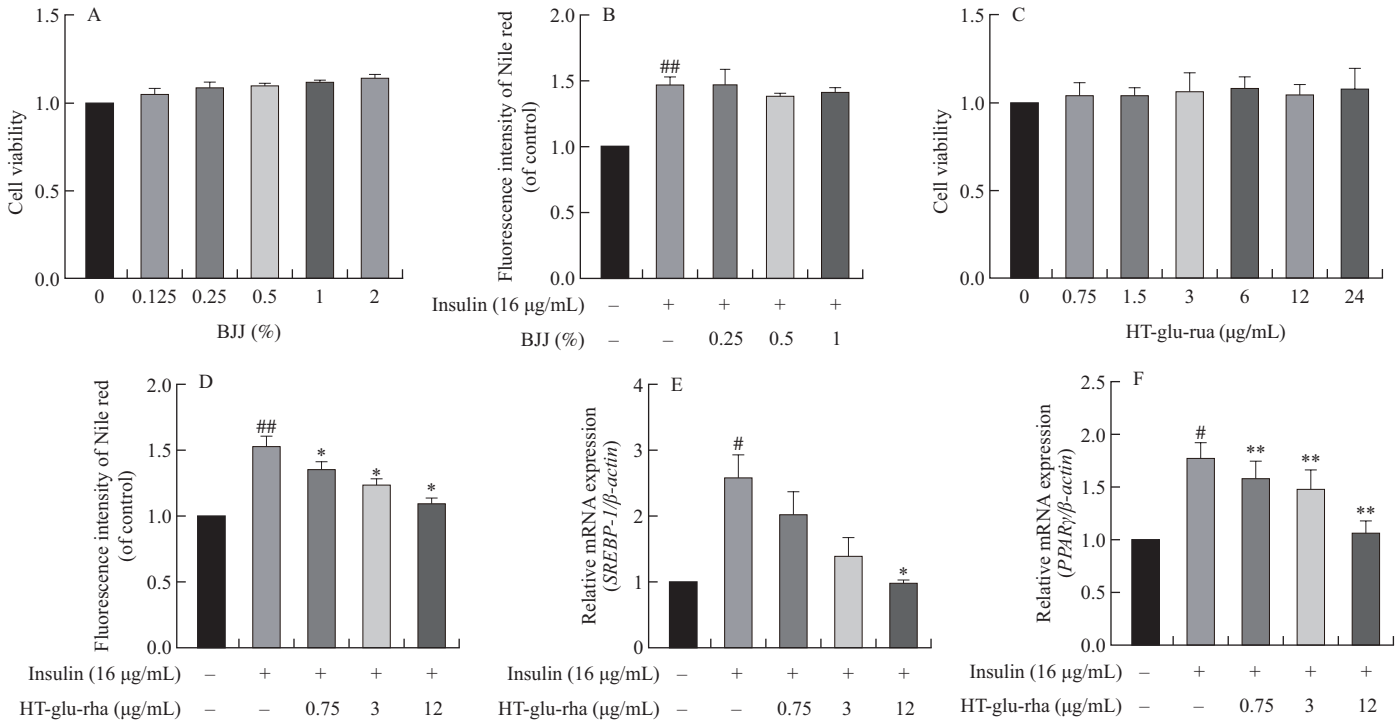

Fig. 6 HT-glu-rha inhibited insulin-induced lipid synthesis in sebocytes. Cell viability after BJJ (A) and HT-glu-rha (C) treatment was determined by the CCK8 assay. Neutral lipid contents were measured by flow cytometry after BJJ (B) and HT-glu-rha (D) treatments. RT-qPCR was conducted to measure the mRNA levels of *SREBP-1* (E) and *PPARγ* (F) in insulin-induced lipid synthesis in sebaceous gland cells after HT-glu-rha treatment. All data were expressed as means ± SEM ($n = 3$). $^{\#}P < 0.05$ and $^{\#\#}P < 0.01$ *vs.* control group, $*P < 0.05$ and $**P < 0.01$ *vs.* insulin-stimulated group.

comparison to insulin-treated sebocytes (Figs. 6E-F). This could explain that the post-fermentation enhanced the effect of inhibiting insulin-stimulated lipid synthesis in sebaceous gland cells.

4. Discussion

The benefits of fermented foods and herbs for overall systemic health are increasingly evident, backed by a growing body of evidence across various studies. Fermentation has the potential to generate and enrich a wide range of bioactive compounds. This process, driven by microorganisms, not only amplifies the original traits of the food but also introduces novel effects or properties[29].

In our research, we've made a novel discovery—during fermentation, the medicinal fungus *B. bassiana* transforms PhGs from Cistanche herbs into smaller polyphenols. The fermentation process occurs in stages: echinacoside is transformed into verbascoside, followed by the metabolism of a portion of verbascoside into HT-glu-rha and caffeic acid, with the latter converting into sulfation of caffeic acid. HT, the mother nucleus structure of HT-glu-rha, is widely recognized as an exceptional antioxidant compound sourced from plants. It possesses anti-inflammatory properties, aids in combating Alzheimer's disease, and inhibits liver lipid synthesis. This component plays a pivotal role in Cistanche's internal metabolism, exerting its medicinal effects. Indeed, while HT itself is quite unstable, HT-glu-rha demonstrates a similar activity to HT while maintaining greater stability, owing to the glycosidic bond linkage. However, studies on the pharmacological activity and pharmacokinetics of HT-glu-rha are quite limited, and we will explore this in more depth in a subsequent study. Interestingly, some of verbascoside was hydroxylated, indicating the potential presence of cytochrome P450 enzymes or polyphenol oxidase in the fermentation broth. This aligns with the *in vivo* metabolism pattern of PhGs, leading to the formation of hydroxylated components[11,30].

PhGs undergo multiple routes of hydrolysis in the gastrointestinal tract and produce degradation intermediates before being absorbed into the blood[31-32]. Indeed, each individual possesses a unique microbiota composition, impacting the bioavailability of PhGs and subsequent production of microbial metabolites, leading to interindividual variability in health effects. Consequently, these effects may not be uniform for everyone. For the first time, we conducted *in vitro* biotransformation of the PhGs, aligning with their metabolism *in vivo*. This process holds the potential to address the variability in the effects of PhGs observed in different individuals.

Acne vulgaris is one of the most common dermatologic conditions globally which is closely related to Western diet[33]. Diet-triggered insulin or insulin-like growth factor activation of the mammalian target of rapamycin complex 1 (mTORC1) is associated with acne. mTORC1 is responsible for sebaceous gland hyperproliferation, lipid synthesis, and keratinocyte hyperplasia in acne cases[34]. *P. acnes* flourishes when sebum production increases[35]. It triggers inflammatory responses by stimulating the production of molecules associated with inflammation, including Toll like receptors (TLR), matrix metalloproteinases (MMP), and inflammatory cytokines[36]. Our research revealed that heat-killed *P. acnes* irritated HaCaT increased IL-1α and IL-6 expression, while PHG and BJJF showed a dose-dependent suppression of these cytokines in the HaCaT cells. Interestingly, higher doses of BJJF exhibited notably superior effects in reducing ROS production induced by *P. acnes* in HaCaT cells, possibly due to the increased likelihood of small-molecule polyphenols to penetrate cell membranes and exert biological activities. Moreover, in insulin-stimulated sebocytes, unlike PHG, BJJF demonstrated a dose-dependent reduction in lipid synthesis. Additionally, HT-glu-rha exhibited similar reductions in lipid synthesis in insulin-stimulated sebocytes by down-regulating the gene expression of *SREBP-1* and *PPARγ* in a dose-dependent manner. However, further studies such as toxicological and pharmacokinetic on our samples are needed before they can be developed into active materials for topical or oral use. In addition, although we performed the fermentation in laboratory conical flasks, further experimental scale-up is required to assess its potential for industrial production.

5. Conclusions

Fermentation of Cistanche extract by *B. bassiana* metabolized the PhGs into small polyphenols, especially HT-glu-rha, enhancing its antioxidant and lipid inhibitory activities. Given the potent bioenzymatic activity of *B. bassiana,* it would be worthwhile to further explore its use in the fermenting hard-to-absorb foods and herbs to enhance their activity and utilization.

Conflict of interest

No conflict of interest exits in the submission of this manuscript, and manuscript is approved by all authors for publication, the work described was original research that has not been published previously, and not under consideration for publication elsewhere, in whole or in part. The study design was approved by the appropriate ethics review board.

Acknowledgments

This research was supported by the Start-up Fund of China Pharmaceutical University (3150020057).

References

[1] H.M. Shi, J. Wang, M.Y. Wang, et al., Identification of cistanche species by chemical and inter-simple sequence repeat fingerprinting, Biol. Pharm. Bull. 32 (2009) 142-146. https://doi.org/10.1248/bpb.32.142.

[2] K.W. Zeng, J.K. Wang, L.C. Wang, et al., Small molecule induces mitochondrial fusion for neuroprotection *via* targeting CK2 without affecting its conventional kinase activity, Signal Transduct Target Ther. 6 (2021) 71. https://doi.org/10.1038/s41392-020-00447-6.

[3] S. Tian, M.S. Miao, X.M. Li, et al., Study on neuroendocrine-immune function of phenylethanoid glycosides of desertliving cistanche herb in perimenopausal rat model, J. Ethnopharmacol. 238 (2019) 111884. https://doi.org/10.1016/j.jep.2019.111884.

[4] K. Zhang, X. Ma, W. He, et al., Extracts of *Cistanche deserticola* can antagonize immunosenescence and extend life span in senescence-accelerated mouse prone 8 (SAM-P8) mice, Evid. Based Complementary Altern. Med. 2014 (2014) 601383. https://doi.org/10.1155/2014/601383.

[5] L. Yang, S. Ding, B. Zhang, et al., Beneficial effects of total phenylethanoid glycoside fraction isolated from *Cistanche deserticola* on bone microstructure in ovariectomized rats, Oxid. Med. Cell Longev. 2019 (2019) 2370862. https://doi.org/10.1155/2019/2370862.

[6] D. Feng, S.Q. Zhou, Y.X. Zhou, et al., Effect of total glycosides of *Cistanche deserticola* on the energy metabolism of human HepG2 cells, Front. Nutr. 10 (2023) 1117364. https://doi.org/10.3389/fnut.2023.1117364.

[7] Y. Jiang, P.F. Tu, Analysis of chemical constituents in *Cistanche* species, J. Chromatogr. A. 1216 (2009) 1970-1979. https://doi.org/10.1016/j.chroma.2008.07.031.

[8] C. Jia, H. Shi, X. Wu, et al., Determination of echinacoside in rat serum by reversed-phase high-performance liquid chromatography with ultraviolet detection and its application to pharmacokinetics and bioavailability, J. Chromatogr. B. 844 (2006) 308-313. https://doi.org/10.1016/j.jchromb.2006.07.040.

[9] J.K. Nicholson, E. Holmes, I.D. Wilson, Gut microorganisms, mammalian metabolism and personalized health care, Nat. Rev. Microbiol. 3 (2005) 431-438. https://doi.org/10.1038/nrmicro1152.

[10] Y. Li, G. Zhou, S. Xing, et al., Identification of echinacoside metabolites produced by human intestinal bacteria using ultraperformance liquid chromatography-quadrupole time-of-flight mass spectrometry, J. Agric. Food Chem. 63 (2015) 6764-6771. https://doi.org/10.1021/acs.jafc.5b02881.

[11] Y. Wang, H. Hao, G. Wang, et al., An approach to identifying sequential metabolites of a typical phenylethanoid glycoside, echinacoside, based on liquid chromatography-ion trap-time of flight mass spectrometry analysis, Talanta 80 (2009) 572-580. https://doi.org/10.1016/j.talanta.2009.07.027.

[12] Q. Cui, Y. Pan, X. Xu, et al., The metabolic profile of acteoside produced by human or rat intestinal bacteria or intestinal enzyme *in vitro* employed UPLC-Q-TOF-MS, Fitoterapia. 109 (2016) 67-74. https://doi.org/10.1016/j.fitote.2015.12.011.

[13] Q. Xu, X. Fang, D. Chen, Pharmacokinetics and bioavailability of ginsenoside Rb1 and Rg1 from *Panax notoginseng* in rats, J. Ethnopharmacol. 84 (2003) 187-192. https://doi.org/10.1016/s0378-8741(02)00317-3.

[14] A. König, N. Sadova, M. Dornmayr, et al., Combined acid hydrolysis and fermentation improves bioactivity of citrus flavonoids *in vitro* and *in vivo*, Commun. Biol. 6 (2023) 1083. https://doi.org/10.1038/s42003-023-05424-7.

[15] M. Hu, Z. Yu, J. Wang, et al., Traditional uses, origins, chemistry and pharmacology of *Bombyx batryticatus*: a review, Molecules 22 (2017) 1779. https://doi.org/10.3390/molecules22101779.

[16] G. Zimmermann, Review on safety of the entomopathogenic fungi *Beauveria bassianaand* and *Beauveria brongniartii*, Biocontrol. Sci. Technol. 17 (2007) 553-596. https://doi.org/10.1080/09583150701309006.

[17] L. Qiao, D. Xie, Q. Liu, et al., Microbial transformation of lovastatin by *Beauveria bassiana*, Acta Pharm. Sin. B. 2 (2012) 300-305. https://doi.org/10.1016/j.apsb.2012.04.001.

[18] Q. Wu, J. Patocka, K. Kuca, Beauvericin, a fusarium mycotoxin: anticancer activity, mechanisms, and human exposure risk assessment, Mini. Rev. Med. Chem. 19 (2019) 206-214. https://doi.org/10.2174/1389557518666180928161808

[19] C. Rabhi, G. Arcile, L. Cariel, et al., Antiangiogenic-like properties of fermented extracts of ayurvedic medicinal plants, J. Med. Food. 18 (2015) 1065-1072. https://doi.org/10.1089/jmf.2014.0128.

[20] Y.Y. Wang, A.R. Ryu, S. Jin, et al., Chlorin e6-mediated photodynamic therapy suppresses *P. acnes*-induced inflammatory response *via* NFκB and MAPKs signaling pathway, PLoS ONE 12 (2017) e0170599. https://doi.org/10.1371/journal.pone.0170599.

[21] Z. Li, L. Ryenchindorj, B. Liu, et al., Chemical profiles and metabolite study of raw and processed *Cistanche deserticola* in rats by UPLC-Q-TOF-MSE, Chinese Med. 16 (2021) 93. https://doi.org/10.1186/s13020-021-00508-0.

[22] R. Ullrich, M. Hofrichter, Enzymatic hydroxylation of aromatic compounds, Cell Mol. Life Sci. 64 (2007) 271-293. https://doi.org/10.1007/s00018-007-6362-1.

[23] H.J. Zeng, Q.Y. Li, J. Ma, et al., A comparative study on the effects of resveratrol and oxyresveratrol against tyrosinase activity and their inhibitory mechanism, Spectrochim. Acta A Mol. Biomol. Spectrosc. 251 (2021) 119405. https://doi.org/10.1016/j.saa.2020.119405.

[24] W. Wang, R. Yang, H. Yao, et al., Inhibiting the formation of advanced glycation end-products by three stilbenes and the identification of their adducts, Food Chem. 295 (2019) 10-15. https://doi.org/10.1016/j.foodchem.2019.02.137.

[25] Y. Yang, G. Zhang, C. Li, et al., Metabolic profile and structure-activity relationship of resveratrol and its analogs in human bladder cancer cells, Cancer Manag. Res. 11 (2019) 4631-4642. https://doi.org/10.2147/cmar.S206748.

[26] L. Hu, X. Sui, X. Dong, et al., Low beauvericin concentrations promote PC-12 cell survival under oxidative stress by regulating lipid metabolism and PI3K/AKT/mTOR signaling, Ecotoxicol. Environ. Saf. 269 (2024) 115786. https://doi.org/10.1016/j.ecoenv.2023.115786.

[27] Y. Fan, X. Liu, N. Keyhani, et al., Regulatory cascade and biological activity of *Beauveria bassiana* oosporein that limits bacterial growth after host death, Proc. Natl. Acad. Sci. U.S.A. 114 (2017) E1578-E1586. https://doi.org/10.1073/pnas.1616543114.

[28] A. Jain, E. Basal, Inhibition of *Propionibacterium acnes*-induced mediators of inflammation by Indian herbs, Phytomedicine 10 (2003) 34-38. https://doi.org/10.1078/094471103321648638.

[29] A. Mukherjee, S. Breselge, E. Dimidi, et al., Fermented foods and gastrointestinal health: underlying mechanisms, Nat. Rev. Gastroenterol. Hepatol. 4 (2023) 248-266. https://doi.org/10.1038/s41575-023-00869-x.

[30] H. Qian, F.J. Yu, D.Y. Lu, et al., Identification of poliumoside metabolites in rat plasma, urine, bile, and intestinal bacteria with UPLC/Q-TOF-MS, Chin. J. Nat. Med. 16 (2018) 871-880. https://doi.org/10.1016/s1875-5364(18)30129-8.

[31] S. Hurst, C.M. Loi, J. Brodfuehrer, et al., Impact of physiological, physicochemical and biopharmaceutical factors in absorption and metabolism mechanisms on the drug oral bioavailability of rats and humans, Expert. Opin. Drug Metab. Toxicol. 3 (2007) 469-489. https://doi.org/10.1517/17425225.3.4.469.

[32] Y. Li, Y. Peng, M. Wang, et al., Rapid screening and identification of the differences between metabolites of *Cistanche deserticola* and *C. tubulosa* water extract in rats by UPLC-Q-TOF-MS combined pattern recognition analysis, J. Pharm. Biomed. Anal. 131 (2016) 364-372. https://doi.org/10.1016/j.jpba.2016.09.018.

[33] L. Cordain, S. Lindeberg, M. Hurtado, et al., Acne vulgaris: a disease of Western civilization, Arch. Dermatol. 138 (2002) 1584-1590. https://doi.org/10.1001/archderm.138.12.1584.

[34] B. Melnik, Dietary intervention in acne: attenuation of increased mTORC1 signaling promoted by Western diet, Dermatoendocrinol. 4 (2012) 20-32. https://doi.org/10.4161/derm.19828.

[35] K.J. McGinley, G.F. Webster, M.R. Ruggieri, et al., Regional variations in density of cutaneous propionibacteria: correlation of *Propionibacterium acnes* populations with sebaceous secretion, J. Clin. Microbiol. 12 (1980) 672-675. https://doi.org/10.1128/jcm.12.5.672-675.1980.

[36] J. Kim, Review of the innate immune response in acne vulgaris: activation of Toll-like receptor 2 in acne triggers inflammatory cytokine responses, Dermatology 211 (2005) 193-198. https://doi.org/10.1159/000087011.